doi: 10.18323/2782-4039-2023-4-66-7

Simulation of electrical parameters of a galvanic cell in the process of microarc oxidation

Ekaterina A. Pecherskaya[1], Doctor of Sciences (Engineering), Professor,
Head of Chair "Information and Measuring Equipment and Metrology"
Anatoly D. Semenov, Doctor of Sciences (Engineering),
professor of Chair "Information and Measuring Equipment and Metrology"
Pavel E. Golubkov*[2], PhD (Engineering),
assistant professor of Chair "Information and Measuring Equipment and Metrology"
Penza State University, Penza (Russia)

***E-mail: iit@pnzgu.ru, golpavpnz@yandex.ru**

[1]ORCID: https://orcid.org/0000-0001-5657-9128
[2]ORCID: https://orcid.org/0000-0002-4387-3181

Received 26.06.2023 *Accepted 11.12.2023*

Abstract: Microarc oxidation is a promising technology for producing wear-resistant anticorrosive coatings for goods made of valve metals and alloys and is used in many industries. One of the main problems of this technology is low controllability caused by the complexity and interconnectedness of physical and chemical phenomena occurring during the coating process. To solve such problems, digital twins are currently actively used. The paper covers the development of mathematical models that are advisable to use as structural elements of the digital twin of the microarc oxidation process. An equivalent electrical circuit of a galvanic cell of microarc oxidation is given, which takes into account the electrolyte resistance, the part coating resistance in the form of a parallel connection of nonlinear active resistance and capacitive reactance. The authors propose a mathematical model describing the behaviour of the equivalent electrical circuit of a galvanic cell of microarc oxidation. A technique for determining the parameters of this model was developed, including the construction of a waveform of changes in the resistance of the cell and its approximation, estimation of the values of resistances and capacitance of the galvanic cell equivalent circuit. The authors proposed a calculation method and developed a Simulink model of the microarc oxidation process, which allows simulating the current and voltage waveforms of a galvanic cell. The analysis of the model showed that the model is stable, controllable and observable, but poorly conditioned, which leads to modelling errors, the maximum value of which is 7 % for voltage and 10 % for current. By the parametric identification method using experimental current and voltage waveforms, the dependences of the parameters of the galvanic cell equivalent circuit on the oxidation time are obtained. It is found that the change in the period average of the galvanic cell active resistance correlates with the coating thickness.

Keywords: microarc oxidation; equivalent electrical circuit; mathematical model; Simulink model; coating resistance and capacitance; model adequacy.

Acknowledgments: This work was supported by the Ministry of Science and Higher Education of the Russian Federation, project No. 1022041100284-5-2.3.1.

The paper was written on the reports of the participants of the XI International School of Physical Materials Science (SPM-2023), Togliatti, September 11–15, 2023.

For citation: Pecherskaya E.A., Semenov A.D., Golubkov P.E. Simulation of electrical parameters of a galvanic cell in the process of microarc oxidation. *Frontier Materials & Technologies*, 2023, no. 4, pp. 73–85. DOI: 10.18323/2782-4039-2023-4-66-7.

INTRODUCTION

Microarc oxidation (MAO) is used to improve the mechanical and physicochemical properties of the surfaces of parts made of aluminium alloys. The process is applicable both to aluminium and to other valve group metals, such as Ti, Zr, Mg, and Ta. The combination of high microhardness and wear resistance with corrosion resistance of coatings produced by the MAO method ensures the widespread application of products with such coatings in many industries [1; 2]. However, at present there are a number of unresolved issues hindering the MAO technology development, the main of which are high energy consumption [3; 4], and low controllability of the technological process, associated with the combined influence of many different factors on the properties of the formed coatings [5; 6].

Currently, one of the promising ways to manage complex production processes is the use of digital twins, which allows simulating and predicting the behaviour of a real object in the virtual world, using information received from sensors on the object throughout its entire life cycle. In this case, as a rule, models of real system components are known or easily created using CAD systems, such as, for example, 3D models in mechanical engineering production [7]. However, for complex multifactor technological processes, such as MAO, the process of creating a digital twin is significantly complicated due to the imperfection or absence of mathematical models of some physical phenomena, leading to the formation of oxide coatings. Many works are concerned with the study of the mechanism of coating formation during MAO [8; 9], however, only some of them provide its analytical description. Thus, in the review paper [10] dealing with the MAO of titanium alloys, there is

a sufficiently detailed mathematical interpretation of the mechanism of electrolysis at high voltage, but microplasma processes are not considered. The work [11] gives formulas for calculating the electron temperature of microdischarge plasma during MAO under the local thermodynamic equilibrium conditions, but no relationship with electrochemical processes is traced. Moreover, according to [10; 12], the fundamental theory of plasma electrolysis containing an analytical description of different phenomena (electrochemical, microplasma, etc.) occurring in the process of MAO as a single interconnected system, has not currently been developed.

Thus, an urgent scientific task is to build a mathematical model that could serve as the basis for a digital twin of the MAO process. At a first approximation, this model should estimate the thickness of the formed coatings based on the hidden information contained in the waveforms of current and voltage measured during the MAO process, by identifying the parameters of the galvanic cell equivalent circuit.

The purpose of the study is to identify the parameters of the equivalent electrical circuit of a galvanic cell, that correlate with the thickness of MAO coatings, and to develop a methodology for determining these parameters.

METHODS

During the study, 30 samples of MAO coatings were produced on blanks made of AD31 commercially pure aluminium, GOST 4784-97 (2000) (Table 1), with the dimensions of 20×15×2 mm. The MAO coatings were formed using an automated MAO installation developed by the authors containing a technological current source, measuring channels for current, voltage and electrolyte temperature, and a control module based on a microcontroller. The technological current source of this system is a series connection of a bank of capacitors with adjustable capacitance and a galvanic cell. The technological current source is powered by sinusoidal voltage from a 220 V 50 Hz mains. Before starting the MAO process, the amplitude value of the current through the galvanic cell was set by changing the capacitor bank capacitance (connecting the required number of capacitors), which remained constant until the MAO processing completion. MAO was carried out for 30 min at a current density of 5 A/dm^2 in the anodic-cathode mode with the ratio of the anodic, and cathodic current equal to 1, in an electrolyte of the NaOH (2 g/l), Na_2SiO_3 (9 g/l) composition, and the first sample was processed for 1 min, the second – for 2 min, etc. Every minute, waveforms of two periods of the forming voltage and current in the galvanic cell were measured using measuring channels built into the MAO installation, with a relative error of ±0.5 % and a sampling frequency of 128 points per period equal to the supply voltage period (20 ms). The electrolyte temperature, during the coating process did not exceed 30 °C. After processing, samples with MAO coatings were removed from the galvanic cell, washed with distilled water and dried. The thickness of the coatings was measured on transverse sections using a Mitaka PF-60 3D contour measuring station-profilometer. Software processing of the obtained experimental dependencies was carried out in the MATLAB+Simulink environment.

RESULTS

Mathematical model of the microarc oxidation process

Fig. 1 shows a characteristic view of experimentally measured waveforms of the galvanic cell voltage and current. The deviation of the forming voltage from the sinusoidal shape is caused by the supply voltage imperfection, as well as by the one-sided conductivity of the "anode – coating – electrolyte – cathode" system, as a result of which voltage rectification is observed (the so-called "valve effect"). Breaks in the voltage waveforms occurring in the anode half-cycle at a voltage of about 320 and 370 V are associated with the ignition and extinguishing of microdischarges. The difference between the current shape and the sinusoidal one (triangular current pulses in the anode and cathode half-cycles), is caused by the electrical breakdown of the oxide layer, which occurs only at the sinusoid peak, when the voltage on the sample exceeds the breakdown voltage. The nonlinearity of the current-voltage characteristics indicates the nonlinear nature of the coating formation process, and the presence of hysteresis with a characteristic loop indicates the capacitive nature of the load. To construct a mathematical model of the MAO process, we will use the nonlinear electrophysical model developed in [13] in the form of an electrical equivalent circuit of a galvanic cell (Fig. 2).

The electrolyte resistance is simulated by R_1 active resistance, the coating resistance is simulated by a parallel connection of R_2 nonlinear active resistance and C_2 capacitance reactance. C_1 capacitance connected in series with the galvanic cell does not belong to the sample under study, and is intended to simulate the output signal of the technological current source (current limiting in the circuit).

The mathematical model describing the behaviour of the MAO electrical equivalent circuit of the galvanic cell (Fig. 2) is as follows:

$$\begin{cases} \frac{1}{C_1}\int I_1 dt + R_1 I_1 + R_2\left(U_1\right) I_2 = U \\ \frac{1}{C_2}\int I_3 dt - R_2\left(U_1\right) I_2 = 0 \\ U_1 = U - \frac{1}{C_1}\int I_1 dt \\ I_1 = I_2 + I_3 \end{cases}. \quad (1)$$

Let us change a model (1) to a state space model:

$$\begin{cases} \frac{d\mathbf{x}}{dt} = \mathbf{A}\mathbf{x} + \mathbf{B}U \\ y = \mathbf{C}\mathbf{x} + \mathbf{D}U \end{cases}, \quad (2)$$

where $\mathbf{x} = \begin{pmatrix} I_1 & I_2 \end{pmatrix}^T$;

$y = I_1 + \frac{U}{R_1}$;

$$\mathbf{A} = \begin{pmatrix} -\frac{C_1 + C_2}{C_1 C_2 R_1} & \frac{1}{C_2 R_1} \\ \frac{1}{C_2 R_2} & -\frac{1}{C_2 R_2} \end{pmatrix};$$

$$\mathbf{B} = \begin{pmatrix} \frac{1}{R_1} \\ 0 \end{pmatrix};$$

$$\mathbf{C} = \begin{pmatrix} 0 & 1 \end{pmatrix};$$

$$\mathbf{D} = 0; R_2 = f\left(U_1\right).$$

Let us estimate the parameters of the model of the MAO electrical equivalent circuit of the galvanic cell. Three equivalent circuit parameters are evaluated: the R_1 electrolyte active resistance, the R_2 nonlinear active resistance of the coating and its C_2 equivalent capacitance.

Since the model is nonlinear, the use of traditional identification methods is impractical and can lead to unacceptable errors in determining the model parameters. In this regard, the authors propose a sequential procedure for determining the model parameters.

1. Construction of a waveform of changes in cell resistance and its approximation. To construct a waveform of changes in cell resistance, we find the derivative of the current-voltage characteristics:

Table 1. *AD31 alloy composition*
Таблица 1. *Состав сплава АД31*

Element	Si	Fe	Cu	Mn	Mg	Cr	Zn	Ti	Others	Al
Content, wt. %	0.2–0.6	0.5	0.1	0.1	0.45–0.9	0.1	0.2	0.15	0.15	The rest

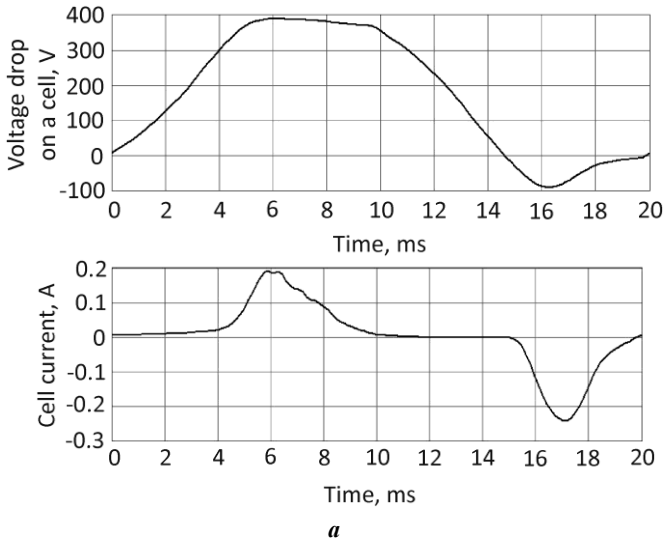

a

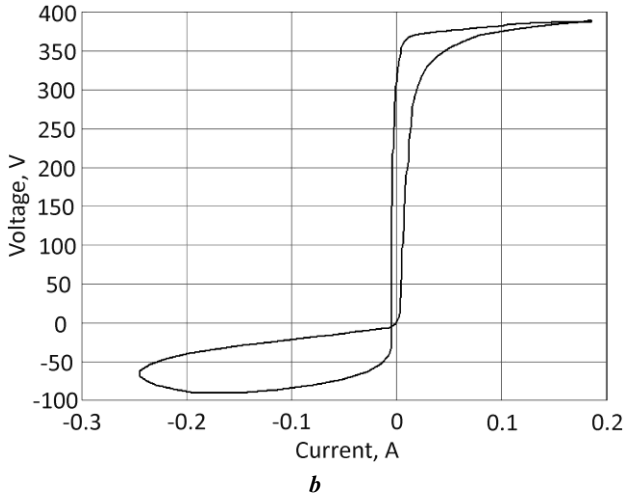

b

Fig. 1. *Waveforms of voltage and current of a galvanic cell (**a**) and its current-voltage characteristics (**b**)*
Рис. 1. *Осциллограммы напряжения и тока гальванической ячейки (**a**) и ее вольтамперная характеристика (**b**)*

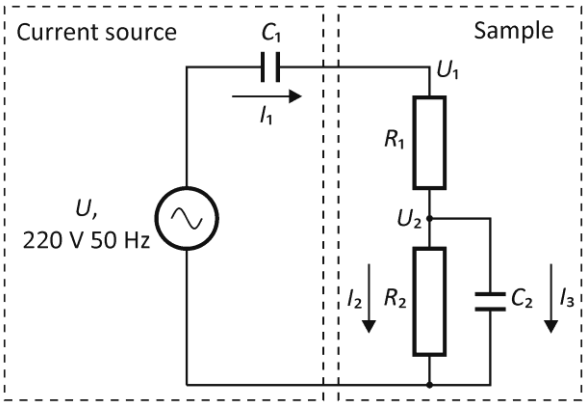

Fig. 2. *An equivalent electrical circuit of the MAO process*
Рис. 2. *Электрическая схема замещения процесса МДО*

$$R_1 + R_2 \approx \frac{\Delta U_1}{\Delta I_1}. \quad (3)$$

Fig. 3 shows waveforms of U_1 voltage, I_1 current and total resistance calculated by formula (3). It can be observed that the waveform of the total resistance of the galvanic cell contains four characteristic sections. In the first section (≈2–7 ms), coating breakdown occurs with a positive half-wave of the voltage applied to it, and the coating resistance sharply drops to a value of the order of 100 Ω. In the second section (≈7–13 ms), the current in the cell changes polarity, and the coating resistance is restored to its original value of approximately 12 kΩ. In the third section (≈13–17 ms), coating breakdown occurs with a negative voltage drop. In the fourth section (≈17–22 ms), the voltage on the cell changes sign and the coating resistance is restored.

It is known that the electrolyte specific conductivity lies in the range of 6.75...22.5 mS·cm^{-1} [14]. Assuming that the R_1 electrolyte resistance remains constant, one can consider that the coating resistance nonlinearly depends on the voltage applied to it and the current flowing through it.

The resulting waveforms allow finding the dependence R_1+R_2=$f(U_1)$, which is shown in Fig. 4. The values of the approximating curve of the dependence of the cell resistance on the voltage applied to it are summarised in Table 2.

Fig. 5 shows the approximation of the calculated cell resistance curve presented in Table 2 by a cosine equation

$$R_1 + R_2 = 70 \cdot \left(1 - \cos\left(\frac{U_1 - 150}{96}\right)\right).$$

2. Estimation of the value of R_1 and R_2 resistances. Taking into account that after the breakdown the R_2 coating resistance is close to zero, the estimate of R_1 will be

$$R_1 = \min\left(\mathbf{R}_{\text{п}}\right), \quad (4)$$

where $\boldsymbol{R}_{im}$ is the set of galvanic cell impedances formed in the coating breakdown areas.

Fig. 6 shows areas of cell low resistance corresponding to time intervals from 2 to 7 ms and from 13 to 17 ms (see Fig. 3). The average resistance value in these sections is R_{2l}=163 Ω, which is an estimate of the R_2 low resistance value. An estimate of the high value of R_2 resistance can be the average value of the resistances taken from Table 2, which corresponds to the value of R_{2h}=5.9 kΩ. In accordance with (4), the estimate of the R_1 electrolyte resistance will be equal to R_1=22 Ω.

3. Estimation of the C_2 cell capacitance value. To estimate C_2, write an expression for the conductivity transfer function. From (1), it follows that

$$W(p) = \frac{I_1(p)}{U_1(p)} = \frac{R_2 C_2 p + 1}{R_1 R_2 C_2 p + R_1 + R_2}. \quad (5)$$

Using the MATLAB System Identification Toolbox application, let us find the parameters of the cell conductivity transfer function. As a result, the following time constants of the transfer function were obtained:

$$\begin{matrix} T_1 = R_1 R_2 C_2 = 0{,}002417 \text{ s} \\ T_2 = R_2 C_2 = 0{,}0009829 \text{ s} \end{matrix}. \quad (6)$$

Let us take the value of R_2 resistance equal to its average value over the period of supply voltage R_{2av}=4.4 kΩ. Then, according to (6), the estimate of C_2 capacitance will be equal to C_2=0.22 μF.

Calculation of time and frequency characteristics of the model of the microarc oxidation process

From knowing the estimate of the model parameters (2), it is easy to calculate its time and frequency characteristics, using the MATLAB Control System Toolbox application. The main characteristics of the linearised model of the MAO process were calculated for the coating breakdown (short-circuit) and open-circuit modes, when the coating resistance is high (Fig. 7).

The transfer functions of conductivity with respect to I_2 current have the form:

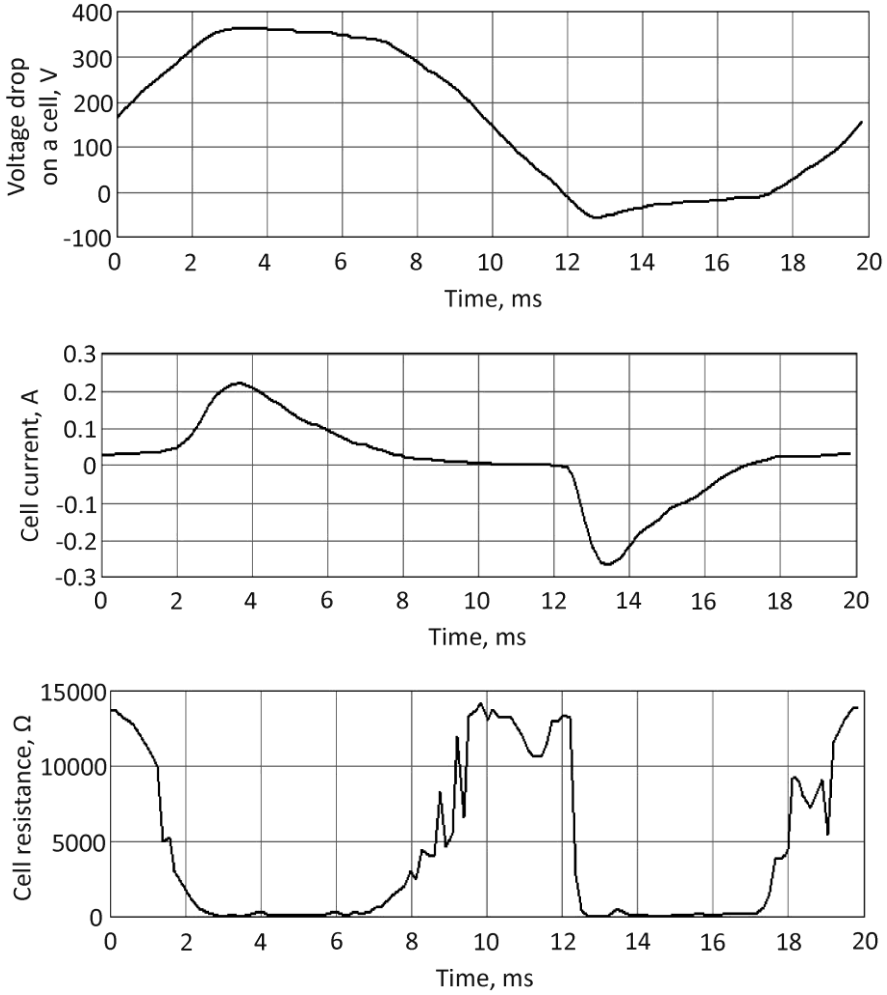

Fig. 3. *Waveforms of voltage, current and resistance of a galvanic cell*
Рис. 3. *Осциллограммы напряжения, тока и сопротивления гальванической ячейки*

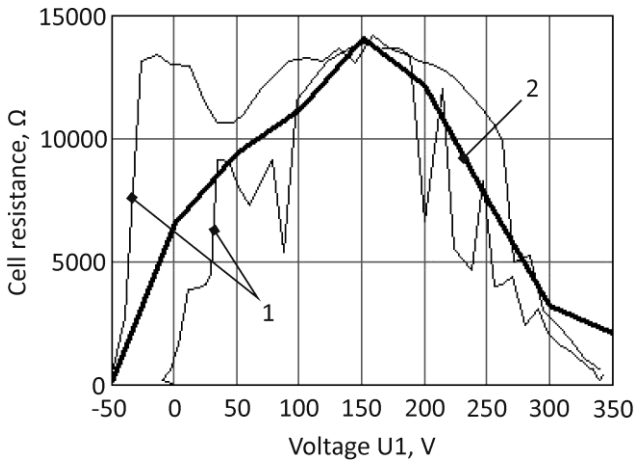

Fig. 4. *Dependences of cell resistance on voltage applied to it*
Рис. 4. *Зависимости сопротивления ячейки от приложенного к ней напряжения*

Table 2. *Approximating curve values*
Таблица 2. *Значения аппроксимирующей кривой*

Voltage, V	−100	−50	0	50	100	150	200	250	300	350	400
Resistance, kΩ	0.15	0.15	6.6	9.4	11.2	14.1	12.2	7.5	3.2	2.1	0.15

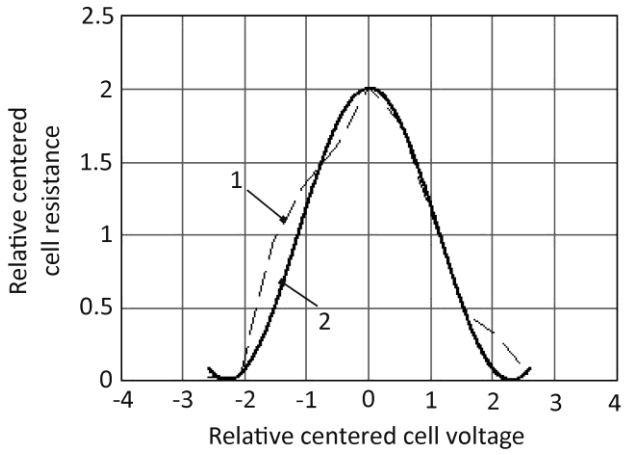

Fig. 5. *Approximation of the calculated curve of cell resistance by the cosine equation*
Рис. 5. *Аппроксимация расчетной кривой сопротивления ячейки уравнением косинуса*

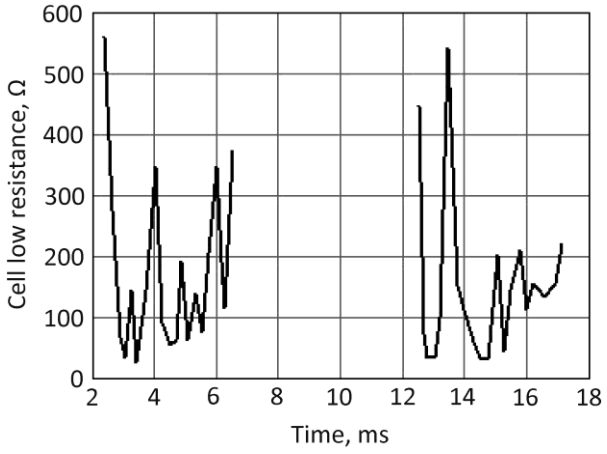

Fig. 6. *Cell low resistance areas*
Рис. 6. *Участки низкого сопротивления ячейки*

$$w_{i2} = \frac{46,957 \cdot s}{\left(s + 2,179 \cdot 10^5\right)\left(s + 48,97\right)};$$

$$w_{i2k} = \frac{46,957 \cdot \left(s - 5,639 \cdot 10^6\right)}{\left(s + 2,436 \cdot 10^5\right)\left(s + 11,82\right)},$$

where *k* index indicates the short-circuit model.

The accuracy of determining the parameters of the galvanic cell equivalent circuit using the parametric identification method was assessed in terms of stability, controllability, observability, and conditionality of the model using the time and frequency characteristics of the MAO process model. The authors revealed that the model is stable, since the performance equation roots are negative. The model is controllable and observable, since the ranks of the controllability and observability matrices are equal to the order of the system, but the model is poorly conditioned, which can

lead to significant errors in its parametric identification. The condition numbers for the open-circuit R_{oc} and short-circuit R_{sc} models are 8410 and 317, respectively. A large value of the model condition number indicates its poor conditioning, i. e., a small change in the input signal can lead to a fairly large change in the output signal, which introduces an error into the modeling results.

Simulation of current and voltage waveforms in the MAO process

The construction of a mathematical model (1) of the MAO process and the assessment of its parameters allow proceeding to modelling the process under consideration. The MAO process modelling was carried out in Simulink. Fig. 8 presents the simulation results. It is found that the maximum voltage modelling error in relation to the U_{max} amplitude value does not exceed 7 %, the maximum current modelling error in relation to the I_{max} amplitude value does not exceed 10 %.

Methodology for determining the significant parameters of the galvanic cell equivalent circuit of the MAO process

Based on the proposed mathematical models, a technique has been developed that allows establishing which parameters of the galvanic cell equivalent circuit change most significantly with increasing coating thickness during the MAO process. The technique is implemented as follows.

1. During the MAO-coating formation, 30 waveforms of the voltage drop and current drop of the galvanic cell are recorded sequentially every minute.

2. In each experiment, $R_{1i}+R_{2i}$ are calculated using formula (3) and the estimate of $R_1=\min(R_{1i}+R_{2i})$ is found.

3. The instantaneous value of R_2 resistance is calculated in each experiment:

$$R_1 + R_{2i} \approx \frac{\Delta U_{1i}}{\Delta I_{1i}}.$$

4. The time dependence of the period average R_2 resistance value is constructed (Fig. 9).

5. In each experiment, using the MATLAB System Identification Toolbox application, the parameters of the transfer function (5) are calculated.

6. Using formulas (6), taking R_2=4400 Ω, the C_2 capacitance, the change graph of which is shown in Fig. 10 is calculated.

DISCUSSION

The developed MAO process models make it possible, using the parametric identification method, to estimate the numerical values of the parameters of the nonlinear electrical equivalent circuit of the galvanic cell, as well as to identify the most significant parameters correlating with the thickness of the coatings.

The nonlinear electrophysical model, used in the calculations in the form of a galvanic cell electrical equivalent circuit is simplified, and does not take into account some features of the process of formation of MAO-coatings. One of the sources of error of a model is the use of ideal C capacitance to simulate the oxide layer, while in electrochemical processes they usually use constant-phase elements CPE, with decomposition into a frequency-independent Q factor, and an n indicator of the degree of heterogeneity of the system [15; 16]. Nevertheless, the model gives satisfactory results (the maximum error in simulating the volt-ampere characteristic is no more than ±7 % for voltage, no more than ±10 % for current), and to a first approximation, can be used to formalise the coating deposition process.

The developed technique for sequential determination of the parameters of the galvanic cell equivalent circuit is physically justified, since the shape of the resulting waveform of changes in the total cell resistance confirms the existing ideas about the MAO process mechanism [17; 18]. For example, Fig. 3 clearly shows areas of the galvanic cell low resistance at maximum anodic and cathodic voltages corresponding to dielectric coating breakdown with subsequent ignition of microdischarges.

As can be observed in Fig. 4, the coating resistance value is 12–15 kΩ. On the other hand, it is known that the impedance modulus of oxide layers on aluminium alloys reaches values of 20–200 MΩ·cm^2, and the polarisation resistance reaches 130–150 MΩ·cm^2 and higher [15; 19]. The revealed discrepancy in the coating resistance values is explained by the fact that the known impedance modulus values were obtained at a low frequency (up to 10 Hz), and in this study the impedance was calculated using the current-voltage characteristics measured at a frequency of 50 Hz. According to available data [16], at this frequency, the coating impedance modulus is of the order of 10^4–10^5 Ω/cm^2, which is consistent with the experimental results.

In the graph of the dependence of the galvanic cell resistance on the forming voltage (Fig. 4), a maximum is observed, the presence of which is determined by the choice of a relatively simple approximating function (cosine equation) and is not associated with physical phenomena occurring in the galvanic cell. The choice of a simple approximating function improves the conditionality of the initially poorly conditioned equation for the MAO process dynamics. In fact, a sharp decrease in the R_2 resistance of the barrier layer is caused by its electrical breakdown by both positive and negative half-waves of the voltage applied to the galvanic cell. During the positive half-cycle, breakdown occurs at a voltage of about +320 V, during the negative half-cycle – about −40 V. Electrical breakdown of the barrier layer at the bottom of the pores when the electrolyte is depleted in ions leads to electrolyte boiling, the appearance of a vapour-gas bubble, and the ignition of a microarc discharge in it. The recovery of the barrier layer resistance is associated with the microarc discharge damping, which occurs because of an increase in the size and the vapour-gas bubble exit beyond the pore, and an accompanying drop in the field strength in it [16; 20]. Thus, the complex form of change in the R_2 barrier layer resistance is caused by a combination of various physical and chemical processes occurring in the pore channels of the barrier layer during the processes of its breakdown and recovery.

Fig. 8 presents the results of modelling the galvanic cell current and voltage waveforms in the Simulink environment. It can be observed that the calculated dependence, well approximates, the experimental curve in the anodic

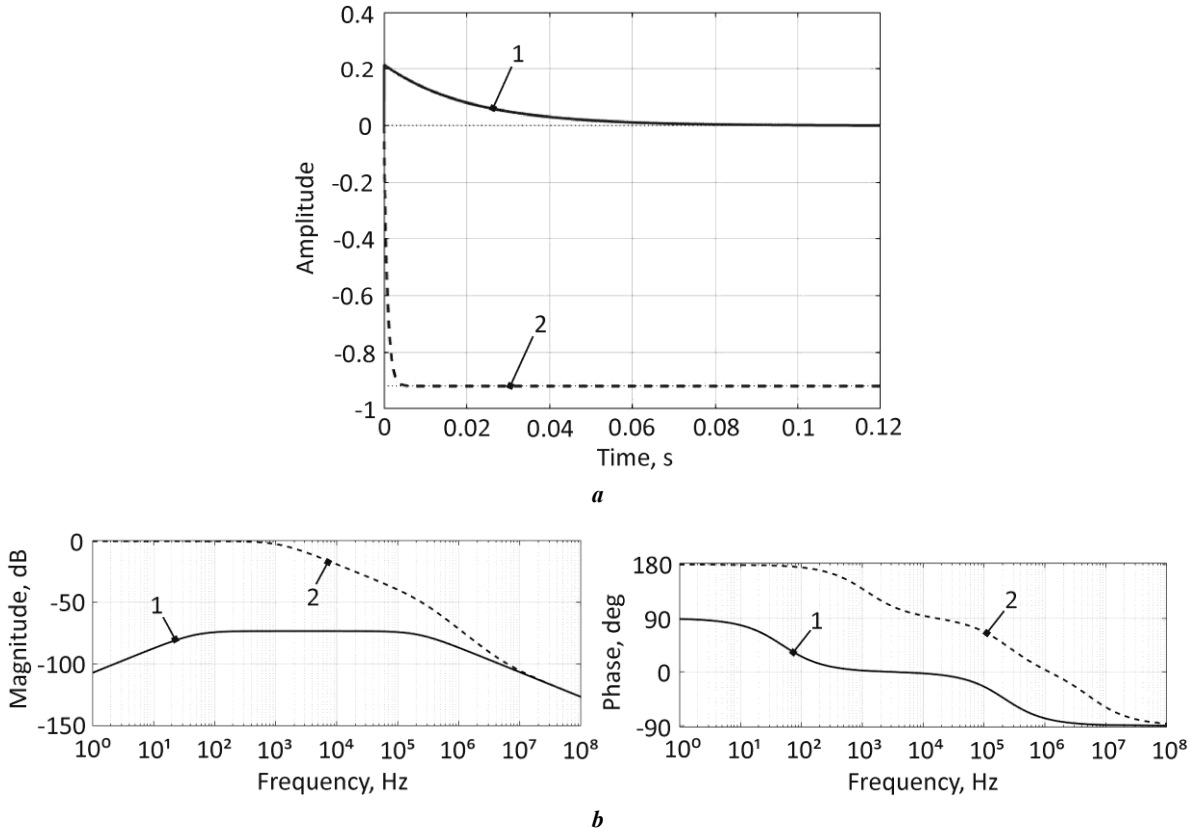

a

b

Fig. 7. *Time (**a**) and frequency characteristics (**b**) of the MAO process model*
Рис. 7. *Временные (**a**) и частотные характеристики (**b**) модели процесса МДО*

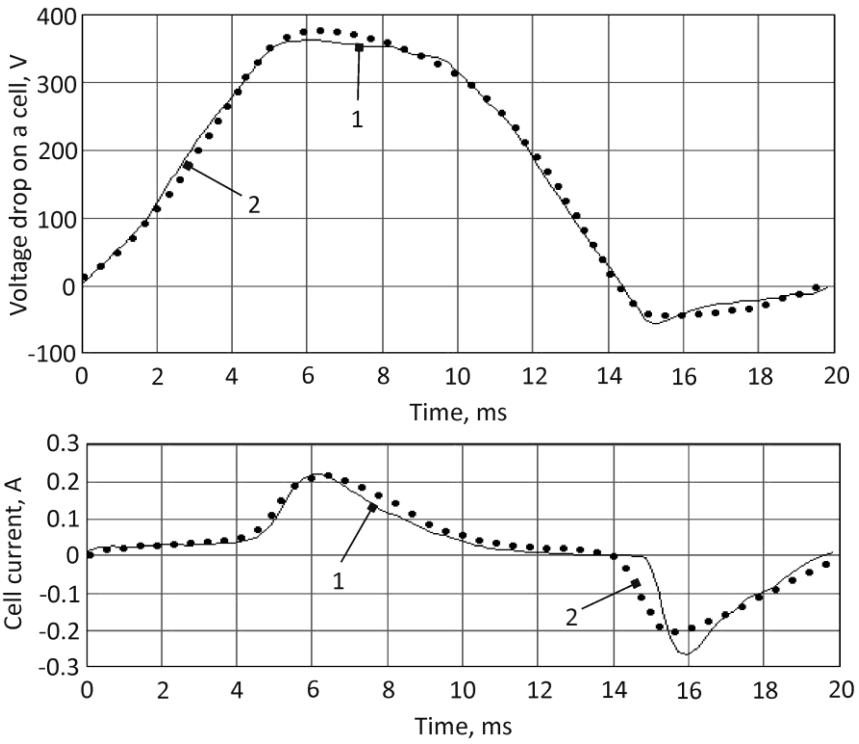

Fig. 8. *Experimental and calculated waveforms of galvanic cell voltage and current*
Рис. 8. *Экспериментальные и расчетные осциллограммы напряжения и тока гальванической ячейки*

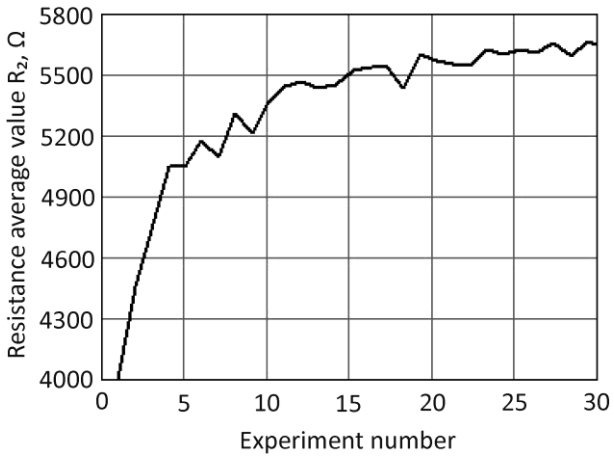

Fig. 9. *Change in the period average value of R_2 resistance in each experiment*
Рис. 9. *Изменение за период среднего значения сопротивления R_2 в каждом опыте*

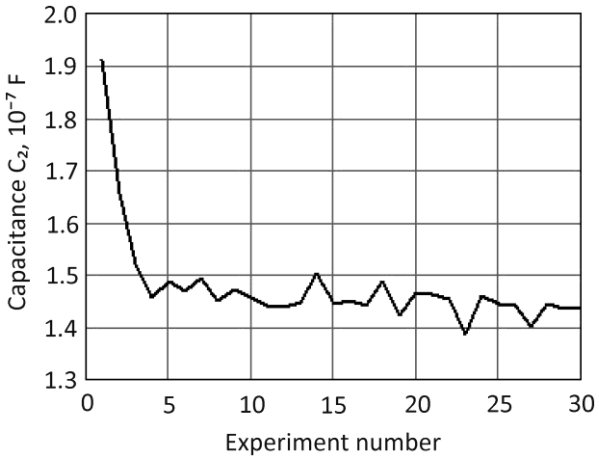

Fig. 10. *Change in capacitance C_2*
Рис. 10. *Изменение емкости C_2*

half-cycle, while in the cathodic half-cycle the discrepancy between these curves becomes significant. This is caused by the fact that the proposed electrical equivalent circuit of a galvanic cell, does not fully reflect the behaviour of a real electrochemical system, as well as by the error of the parametric identification method and the poor conditionality of the model.

Fig. 9 and 10 present the results of applying the developed technique for determining the significant parameters of the galvanic cell equivalent circuit of the MAO process. To identify the degree of relationship between resistance and capacitance and coating thickness, the authors performed a correlation analysis, during which point and interval estimates of the correlation factor were obtained using the Fisher criterion with a confidence probability of 95 %. The results of the correlation analysis are presented in Fig. 11 and Table 3. It can be observed that there is a strong direct correlation between resistance and coating thickness; in the case of capacitance, an inverse correlation occurs, but it is less pronounced (perhaps this is due to the peculiarities of the galvanic cell equivalent circuit and the error of the model). Thus, as a significant parameter for determining the thickness of coatings in the MAO process, it is reasonable to use the coating resistance calculated according to the proposed technique using the current-voltage characteristics of the galvanic cell.

Taking into account the above, the authors can conclude the following. The proposed mathematical model fundamentally provides the ability of determining the thickness of coatings during the MAO process, despite the low accuracy. Moreover, the model allows reproducing waveforms of the galvanic cell current and voltage, which satisfactorily approximate the experimental data. Improving the model taking into account electrochemical impedances will allow improving the simulation accuracy, the result reproducibility and its convergence with experiment, and the use of experimental waveforms from the updated database in calculations, will provide the ability of predicting the thickness of coatings for various MAO processing modes.

Table 3. *Correlation analysis results*
Таблица 3. *Результаты корреляционного анализа*

Coating parameter	Correlation factor	Confidence interval
Resistance	0.968	[0.93; 0.98]
Capacitance	−0.611	[−0.80; −0.30]

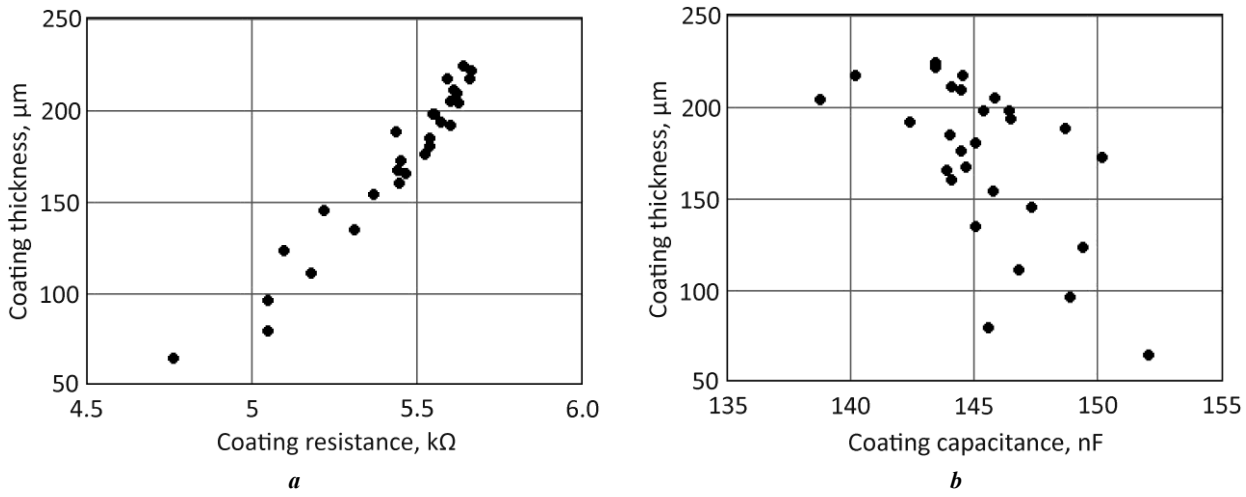

Fig. 11. *Scattering graphs for coating resistance (**a**) and capacitance (**b**)*
Рис. 11. *Диаграммы рассеяния для сопротивления (**a**) и емкости (**b**) покрытия*

The results of the study can be used both in scientific research when developing digital twins and automated control systems for the MAO process, and in production when developing the technology for applying microarc oxide coatings.

CONCLUSIONS

The proposed mathematical model based on the electrical equivalent circuit of a galvanic cell, reflects the relationship between current and voltage in a galvanic cell, and allows simulating current and voltage waveforms during the MAO process with an error of no more than ±10 %. The model is simplified; it does not take into account some physical and chemical laws of the oxide coating formation, which is its disadvantage. Nevertheless, the model has satisfactory accuracy, which allows using the calculation results as an initial approximation, when estimating the electrical parameters of coatings.

The developed technique for identifying the proposed model parameters allows determining the time dependences of the coating resistance, and capacitance during the MAO process using experimentally obtained waveforms of current and voltage in a galvanic cell. Using the correlation analysis method, the degree of relationship between these parameters, and the coating thickness was established. A strong correlation was found between resistance and coating thickness, which allows using the coating resistance as a significant parameter for assessing the thickness of the coating during its formation.

Using the developed identification technique, the parameters of the electrical equivalent circuit of the galvanic cell correlating with the thickness of MAO-coatings were identified.

REFERENCES

1. Yu Ji-Min, Choe Han-Cheol. Morphology Changes and Bone Formation on PEO-treated Ti-6Al-4V Alloy in Electrolyte Containing Ca, P, Sr, and Si Ions. *Applied Surface Science*, 2019, vol. 477, pp. 121–130. DOI: 10.1016/j.apsusc.2017.11.223.
2. Simchen F., Sieber M., Kopp A., Lampke Th. Introduction to Plasma Electrolytic Oxidation – An Overview of the Process and Applications. *Coatings*, 2020, vol. 10, no. 7, article number 628. DOI: 10.3390/coatings10070628.
3. Troughton S.C., Nomine A., Nomine A.V., Henrion G., Clyne T.W. Synchronised electrical monitoring and high speed video of bubble growth associated with individual discharges during plasma electrolytic oxidation. *Applied Surface Science*, 2015, vol. 359, pp. 405–411. DOI: 10.1016/j.apsusc.2015.10.124.
4. Yang Kai, Zeng Jiaquan, Huang Haisong, Chen Jiadui, Cao Biao. A Novel Self-Adaptive Control Method for Plasma Electrolytic Oxidation Processing of Aluminum

Alloys. *Materials*, 2019, vol. 12, no. 17, article number 2744. DOI: 10.3390/ma12172744.
5. Pecherskaya E.A., Golubkov P.E., Karpanin O.V., Artamonov D.V., Safronov M.I., Pecherskiy A.V. Study on Effects of Technological Parameters of Micro-Arc Oxidation on Properties of Oxide Coatings. *Izvestiya vysshikh uchebnykh zavedeniy. Elektronika*, 2019, vol. 24, no. 4, pp. 363–369. DOI: 10.24151/1561-5405-2019-24-4-363-369.
6. Tu Wenbin, Zhu Zhunda, Zhuang Xiujuan, Cheng Yingliang, Skeldon P. Effect of frequency on black coating formation on AZ31 magnesium alloy by plasma electrolytic oxidation in aluminate-tungstate electrolyte. *Surface and Coatings Technology*, 2019, vol. 372, pp. 34–44. DOI: 10.1016/j.surfcoat.2019.05.012.
7. Botin-Sanabria D.M., Mihaita A.-S., Peimbert-Garcia R.E., Ramirez-Moreno M.A., Ramirez-Mendoza R.A., Lozoya-Santos J.J. Digital Twin Technology Challenges and Applications: A Comprehensive Review. *Remote Sensing*, 2022, vol. 14, no. 6, article number 1335. DOI: 10.3390/rs14061335.
8. Zhu Lujun, Ke Xiaoxing, Li Jingwei, Zhang Yuefei, Zhang Zhenhua, Sui Manling. Growth mechanisms for initial stages of plasma electrolytic oxidation coating on Al. *Surfaces and Interfaces*, 2021, vol. 25, article number 101186. DOI: 10.1016/j.surfin.2021.101186.
9. Rogov A.B., Huang Yingying, Shore D., Matthews A., Yerokhin A. Toward rational design of ceramic coatings generated on valve metals by plasma electrolytic oxidation: The role of cathodic polarization. *Ceramics International*, 2021, vol. 47, no. 24, pp. 34137–34158. DOI: 10.1016/j.ceramint.2021.08.324.
10. Aliofkhazraei M., Macdonald D.D., Matykina E., Parfenov E.V., Egorkin V.S., Curran J.A., Troughton S.C., Sinebryukhov S.L., Gnedenkov S.V., Lampke T., Simchen F., Nabavi H.F. Review of plasma electrolytic oxidation of titanium substrates: Mechanism, properties, applications and limitations. *Applied Surface Science Advances*, 2021, vol. 5, article number 100121. DOI: 10.1016/j.apsadv.2021.100121.
11. Hussein R.O., Nie X., Northwood D.O., Yerokhin A., Matthews A. Spectroscopic study of electrolytic plasma and discharging behaviour during the plasma electrolytic oxidation (PEO) process. *Journal of Physics D: Applied Physics*, 2010, vol. 43, no. 10, article number 105203. DOI: 10.1088/0022-3727/43/10/105203.
12. Clyne T.W., Troughton S.C. A review of recent work on discharge characteristics during plasma electrolytic oxidation of various metals. *International Materials Reviews*, 2018, vol. 64, no. 3, pp. 1–36. DOI: 10.1080/09506608.2018.1466492.
13. Golubkov P.E., Pecherskaya E.A., Artamonov D.V., Zinchenko T.O., Gerasimova Yu.E., Rozenberg N.V. Electrophysical model of micro-arc oxidation process. *Russian Physics Journal*, 2020, vol. 62, no. 11, pp. 2137–2144. DOI: 10.1007/s11182-020-01958-z.
14. Mengesha G.A., Chu Jinn P., Lou Bih-Show, Lee Jyh-Wei. Corrosion performance of plasma electrolytic oxidation grown oxide coating on pure aluminum: effect of borax concentration. *Journal of Materials Research and Technology*, 2020, vol. 9, no. 4, pp. 8766–8779. DOI: 10.1016/j.jmrt.2020.06.020.
15. Sowa M., Olesinski A., Szumski B., Maciej A., Bik M., Jelen P., Sitarz M., Simka W. Electrochemical characterization of anti-corrosion coatings formed on 6061 aluminum alloy by plasma electrolytic oxidation in the corrosion inhibitor-enriched aqueous solutions. *Electrochimica Acta*, 2022, vol. 424, article number 140652. DOI: 10.1016/j.electacta.2022.140652.
16. Polunin A.V., Cheretaeva A.O., Borgardt E.D., Rastegaev I.A., Krishtal M.M., Katsman A.V., Yasnikov I.S. Improvement of oxide layers formed by plasma electrolytic oxidation on cast Al-Si alloy by incorporating TiC nanoparticles. *Surface and Coatings Technology*, 2021, vol. 423, article number 127603. DOI: 10.1016/j.surfcoat.2021.127603.
17. Moga S.G., Negrea D.A., Ducu C.M., Malinovschi V., Schiopu A.G., Coaca E., Patrascu I. The Influence of Processing Time on Morphology, Structure and Functional Properties of PEO Coatings on AZ63 Magnesium Alloy. *Applied Sciences*, 2022, vol. 12, no. 24, article number 12848. DOI: 10.3390/app122412848.
18. Mortazavi G., Jiang Jiechao, Meletis E.I. Investigation of the plasma electrolytic oxidation mechanism of titanium. *Applied Surface Science*, 2019, vol. 488, pp. 370–382. DOI: 10.1016/j.apsusc.2019.05.250.
19. Egorkin V.S., Gnedenkov S.V., Sinebryukhov S.L., Vyaliy I.E., Gnedenkov A.S., Chizhikov R.G. Increasing thickness and protective properties of PEO-coatings on aluminum alloy. *Surface and Coatings Technology*, 2018, vol. 334, pp. 29–42. DOI: 10.1016/j.surfcoat.2017.11.025.
20. Kaseem M., Fatimah S., Nashrah N., Ko Young Gun. Recent progress in surface modification of metals coated by plasma electrolytic oxidation: Principle, structure, and performance. *Progress in Materials Science*, 2021, vol. 117, article number 100735. DOI: 10.1016/j.pmatsci.2020.100735.

СПИСОК ЛИТЕРАТУРЫ

1. Yu Ji-Min, Choe Han-Cheol. Morphology Changes and Bone Formation on PEO-treated Ti-6Al-4V Alloy in Electrolyte Containing Ca, P, Sr, and Si Ions // Applied Surface Science. 2019. Vol. 477. P. 121–130. DOI: 10.1016/j.apsusc.2017.11.223.
2. Simchen F., Sieber M., Kopp A., Lampke Th. Introduction to Plasma Electrolytic Oxidation – An Overview of the Process and Applications // Coatings. 2020. Vol. 10. № 7. Article number 628. DOI: 10.3390/coatings10070628.
3. Troughton S.C., Nomine A., Nomine A.V., Henrion G., Clyne T.W. Synchronised electrical monitoring and high speed video of bubble growth associated with individual discharges during plasma electrolytic oxidation // Applied Surface Science. 2015. Vol. 359. P. 405–411. DOI: 10.1016/j.apsusc.2015.10.124.
4. Yang Kai, Zeng Jiaquan, Huang Haisong, Chen Jiadui, Cao Biao. A Novel Self-Adaptive Control Method for Plasma Electrolytic Oxidation Processing of Aluminum Alloys // Materials. 2019. Vol. 12. № 17. Article number 2744. DOI: 10.3390/ma12172744.
5. Печерская Е.А., Голубков П.Е., Карпанин О.В., Артамонов Д.В., Сафронов М.И., Печерский А.В. Исследование влияния технологических параметров процесса микродугового оксидирования на свойства

оксидных покрытий // Известия высших учебных заведений. Электроника. 2019. Т. 24. № 4. С. 363–369. DOI: 10.24151/1561-5405-2019-24-4-363-369.
6. Tu Wenbin, Zhu Zhunda, Zhuang Xiujuan, Cheng Yingliang, Skeldon P. Effect of frequency on black coating formation on AZ31 magnesium alloy by plasma electrolytic oxidation in aluminate-tungstate electrolyte // Surface and Coatings Technology. 2019. Vol. 372. P. 34–44. DOI: 10.1016/j.surfcoat.2019.05.012.
7. Botin-Sanabria D.M., Mihaita A.-S., Peimbert-Garcia R.E., Ramirez-Moreno M.A., Ramirez-Mendoza R.A., Lozoya-Santos J.J. Digital Twin Technology Challenges and Applications: A Comprehensive Review // Remote Sensing. 2022. Vol. 14. № 6. Article number 1335. DOI: 10.3390/rs14061335.
8. Zhu Lujun, Ke Xiaoxing, Li Jingwei, Zhang Yuefei, Zhang Zhenhua, Sui Manling. Growth mechanisms for initial stages of plasma electrolytic oxidation coating on Al // Surfaces and Interfaces. 2021. Vol. 25. Article number 101186. DOI: 10.1016/j.surfin.2021.101186.
9. Rogov A.B., Huang Yingying, Shore D., Matthews A., Yerokhin A. Toward rational design of ceramic coatings generated on valve metals by plasma electrolytic oxidation: The role of cathodic polarization // Ceramics International. 2021. Vol. 47. № 24. P. 34137–34158. DOI: 10.1016/j.ceramint.2021.08.324.
10. Aliofkhazraei M., Macdonald D.D., Matykina E., Parfenov E.V., Egorkin V.S., Curran J.A., Troughton S.C., Sinebryukhov S.L., Gnedenkov S.V., Lampke T., Simchen F., Nabavi H.F. Review of plasma electrolytic oxidation of titanium substrates: Mechanism, properties, applications and limitations // Applied Surface Science Advances. 2021. Vol. 5. Article number 100121. DOI: 10.1016/j.apsadv.2021.100121.
11. Hussein R.O., Nie X., Northwood D.O., Yerokhin A., Matthews A. Spectroscopic study of electrolytic plasma and discharging behaviour during the plasma electrolytic oxidation (PEO) process // Journal of Physics D: Applied Physics. 2010. Vol. 43. № 10. Article number 105203. DOI: 10.1088/0022-3727/43/10/105203.
12. Clyne T.W., Troughton S.C. A review of recent work on discharge characteristics during plasma electrolytic oxidation of various metals // International Materials Reviews. 2018. Vol. 64. № 3. P. 1–36. DOI: 10.1080/09506608.2018.1466492.
13. Голубков П.Е., Печерская Е.А., Артамонов Д.В., Зинченко Т.О., Герасимова Ю.Е., Розенберг Н.В. Электрофизическая модель процесса микродугового оксидирования // Известия высших учебных заведений. Физика. 2019. Т. 62. № 11. С. 166–171. DOI: 10.17223/00213411/ 62/11/166.
14. Mengesha G.A., Chu Jinn P., Lou Bih-Show, Lee Jyh-Wei. Corrosion performance of plasma electrolytic oxidation grown oxide coating on pure aluminum: effect of borax concentration // Journal of Materials Research and Technology. 2020. Vol. 9. № 4. P. 8766–8779. DOI: 10.1016/j.jmrt.2020.06.020.
15. Sowa M., Olesinski A., Szumski B., Maciej A., Bik M., Jelen P., Sitarz M., Simka W. Electrochemical characterization of anti-corrosion coatings formed on 6061 aluminum alloy by plasma electrolytic oxidation in the corrosion inhibitor-enriched aqueous solutions // Electrochimica Acta. 2022. Vol. 424. Article number 140652. DOI: 10.1016/j.electacta.2022.140652.
16. Polunin A.V., Cheretaeva A.O., Borgardt E.D., Rastegaev I.A., Krishtal M.M., Katsman A.V., Yasnikov I.S. Improvement of oxide layers formed by plasma electrolytic oxidation on cast Al-Si alloy by incorporating TiC nanoparticles // Surface and Coatings Technology. 2021. Vol. 423. Article number 127603. DOI: 10.1016/j.surfcoat.2021.127603.
17. Moga S.G., Negrea D.A., Ducu C.M., Malinovschi V., Schiopu A.G., Coaca E., Patrascu I. The Influence of Processing Time on Morphology, Structure and Functional Properties of PEO Coatings on AZ63 Magnesium Alloy // Applied Sciences. 2022. Vol. 12. № 24. Article number 12848. DOI: 10.3390/app122412848.
18. Mortazavi G., Jiechao Jiang, Meletis E.I. Investigation of the plasma electrolytic oxidation mechanism of titanium // Applied Surface Science. 2019. Vol. 488. P. 370–382. DOI: 10.1016/j.apsusc.2019.05.250.
19. Egorkin V.S., Gnedenkov S.V., Sinebryukhov S.L., Vyaliy I.E., Gnedenkov A.S., Chizhikov R.G. Increasing thickness and protective properties of PEO-coatings on aluminum alloy // Surface and Coatings Technology. 2018. Vol. 334. P. 29–42. DOI: 10.1016/j.surfcoat.2017.11.025.
20. Kaseem M., Fatimah S., Nashrah N., Ko Young Gun. Recent progress in surface modification of metals coated by plasma electrolytic oxidation: Principle, structure, and performance // Progress in Materials Science. 2021. Vol. 117. Article number 100735. DOI: 10.1016/j.pmatsci.2020.100735.

Моделирование электрических параметров гальванической ячейки в процессе микродугового оксидирования

Печерская Екатерина Анатольевна[1], доктор технических наук, профессор,
заведующий кафедрой «Информационно-измерительная техника и метрология»
Семёнов Анатолий Дмитриевич, доктор технических наук,
профессор кафедры «Информационно-измерительная техника и метрология»
Голубков Павел Евгеньевич*[2], кандидат технических наук,
доцент кафедры «Информационно-измерительная техника и метрология»
Пензенский государственный университет, Пенза (Россия)

***E-mail: iit@pnzgu.ru, golpavpnz@yandex.ru**

[1]ORCID: https://orcid.org/0000-0001-5657-9128
[2]ORCID: https://orcid.org/0000-0002-4387-3181

Поступила в редакцию 26.06.2023 *Принята к публикации 11.12.2023*

Аннотация: Микродуговое оксидирование является перспективной технологией получения износостойких антикоррозионных покрытий изделий из вентильных металлов и сплавов и применяется во многих отраслях промышленности. Одной из основных проблем данной технологии является низкая управляемость, обусловленная сложностью и взаимосвязанностью физико-химических явлений, происходящих в процессе нанесения покрытий. Для решения подобных проблем в настоящее время активно используются цифровые двойники. Исследование посвящено разработке математических моделей, которые целесообразно использовать в качестве структурных элементов цифрового двойника процесса микродугового оксидирования. Представлена электрическая схема замещения гальванической ячейки микродугового оксидирования, учитывающая сопротивление электролита, сопротивление покрытия детали в виде параллельного соединения нелинейного активного сопротивления и реактивного емкостного сопротивления. Предложена математическая модель, описывающая поведение электрической схемы замещения гальванической ячейки микродугового оксидирования. Разработана методика определения параметров указанной модели, включающая построение осциллограммы изменения сопротивления ячейки и ее аппроксимацию, оценку значений сопротивлений и емкости схемы замещения гальванической ячейки. Предложен способ расчета и разработана Simulink-модель процесса микродугового оксидирования, позволяющая имитировать осциллограммы тока и напряжения гальванической ячейки. Анализ модели показал, что модель устойчива, управляема и наблюдаема, но плохо обусловлена, что приводит к возникновению ошибок моделирования, максимальное значение которых составляет 7 % для напряжения и 10 % для тока. Методом параметрической идентификации с использованием экспериментальных осциллограмм тока и напряжения получены зависимости параметров схемы замещения гальванической ячейки от времени оксидирования. Установлено, что изменение среднего за период активного сопротивления гальванической ячейки коррелирует с толщиной покрытия.

Ключевые слова: микродуговое оксидирование; электрическая схема замещения; математическая модель; Simulink-модель; сопротивление и емкость покрытия; адекватность модели.

Благодарности: Работа выполнена при поддержке Министерства науки и высшего образования РФ, проект № 1022041100284-5-2.3.1.

Статья подготовлена по материалам докладов участников XI Международной школы «Физическое материаловедение» (ШФМ-2023), Тольятти, 11–15 сентября 2023 года.

Для цитирования: Печерская Е.А., Семёнов А.Д., Голубков П.Е. Моделирование электрических параметров гальванической ячейки в процессе микродугового оксидирования // Frontier Materials & Technologies. 2023. № 4. С. 73–85. DOI: 10.18323/2782-4039-2023-4-66-7.